

Listeria-based vaccination against the pericyte antigen RGS5 elicits anti-vascular effects and colon cancer protection

Trevor S. Anderson^a, Amanda L. McCormick^a, Elizabeth A. Daugherty^a, Mariam Oladejo^a, Izuchukwu F. Okpalanwaka^a, Savanna L. Smith^a, Duke Appiah^b, Laurence M. Wood^a, and Devin B. Lowe^a

^aDepartment of Immunotherapeutics and Biotechnology, Jerry H. Hodge School of Pharmacy, Texas Tech University Health Sciences Center, Abilene, TX, USA; ^bDepartment of Public Health, School of Population and Public Health, Texas Tech University Health Sciences Center, Lubbock, TX, USA

ABSTRACT

Colorectal cancer (CRC) remains a leading cause of cancer-related mortality despite efforts to improve standard interventions. As CRC patients can benefit from immunotherapeutic strategies that incite effector T cell action, cancer vaccines represent a safe and promising therapeutic approach to elicit protective and durable immune responses against components of the tumor microenvironment (TME). In this study, we investigate the pre-clinical potential of a *Listeria monocytogenes* (Lm)-based vaccine targeting the CRC-associated vasculature. CRC survival and progression are reliant on functioning blood vessels to effectively mediate various metabolic processes and oxygenate underlying tissues. We, therefore, advance the strategy of initiating immunity in syngeneic mouse models against the endogenous pericyte antigen RGS5, which is a critical mediator of pathological vascularization. Overall, Lm-based vaccination safely induced potent anti-tumor effects that consisted of recruiting functional Type-1-associated T cells into the TME and reducing tumor blood vessel content. This study underscores the promising clinical potential of targeting RGS5 against vascularized tumors like CRC.

ARTICLE HISTORY

Received 28 June 2023
Revised 11 September 2023
Accepted 14 September 2023

KEYWORDS

Anti-angiogenic vaccine;
colon cancer; listeria
monocytogenes; pericyte;
RGS5

Introduction


Colorectal cancer (CRC) represents a substantial threat to global health – with increasing incidence occurring in younger patients.^{1,2} Aggressive chemotherapy complemented with newer approaches like immune checkpoint blockade (ICB) are beginning to attain short-term successes in select individuals with high tumor mutational burden.^{3–5} More established strategies combining chemotherapy with anti-vascular therapies (notably against VEGF and VEGFRs) also demonstrate increased overall survival but are ultimately met with tumor relapse.⁴ Therefore, despite current standards of care, there are unmet needs to improve general patient prognosis and address the approximately 25% of CRC cases that present with advanced disease and yield poor survival rates.⁶

Cancer vaccines offer a promising modality in conveying effective immunotherapy to CRC, particularly alongside ICB.⁷ Vaccines bolster the immune system by generating specific T cell responses and have been traditionally achieved using agents like dendritic cells (DCs) or viral vectors.^{8,9} *Listeria monocytogenes* (Lm)-based vaccines represent an alternative approach and have pre-clinically elicited robust immune responses against tumor-associated antigens (TAAs), leading to improved survival outcomes against tumor types such as breast cancer and renal cell carcinoma.^{10,11} By harnessing the Lm bacterium's ability to preferentially infect antigen presenting cells, such as DCs, TAAs can be directly introduced to DCs,

which subsequently process/present various target-specific epitopes that drive cytotoxic T cell responses.^{12,13} Tumor blood vessel antigens (TBVAs) can also serve as targeting modalities over traditional TAAs given their required and heightened expression in cancer-derived endothelial cells and pericytes.¹⁴ The selective ablation of vascular content also normalizes blood flow dynamics within the tumor microenvironment (TME), permitting greater immune cell recruitment and activity that culminates in reduced cancer growth and regression.^{15,16}

Pericytes are contractile cells that reside on the outer surface of endothelial tubes and are critical to the stability and function of blood vessels. Notably, pericytes are an attractive TME-based immunotherapeutic target since their aberrant expression and behavior support a chaotic tumor-derived blood vessel system that ultimately works to [i] impair drug delivery/action and [ii] augment growth of vascularized cancers such as CRC.¹⁷ Of the various pericyte-derived factors, regulator of G protein signaling 5 (RGS5) is an essential signal transduction molecule during vessel remodeling and is upregulated in the TME during pathological vascularization.^{18,19} The specific ablation of RGS5 has also demonstrated safe and potent anti-tumoral effects both in pre-clinical cancer models^{20–22} and melanoma patients,²³ qualifying it as a relevant TBVA for vaccine purposes. In the current study, we evaluate for the first time the capacity for an Lm-based vaccine to induce potent immune-mediated effects against

CONTACT Laurence M. Wood  laurence.wood@ttuhsc.edu; Devin B., Lowe  devin.lowe@ttuhsc.edu 

 Supplemental data for this article can be accessed online at <https://doi.org/10.1080/2162402X.2023.2260620>

© 2023 The Author(s). Published with license by Taylor & Francis Group, LLC.

This is an Open Access article distributed under the terms of the Creative Commons Attribution-NonCommercial License (<http://creativecommons.org/licenses/by-nc/4.0/>), which permits unrestricted non-commercial use, distribution, and reproduction in any medium, provided the original work is properly cited. The terms on which this article has been published allow the posting of the Accepted Manuscript in a repository by the author(s) or with their consent.

CRC that are characteristic of RGS5 targeting and vascular disruption.

Materials and methods

Mice

Female 6–8-week-old C57BL/6 and BALB/c mice were obtained from The Jackson Laboratory. Animals were housed in micro-isolator cages and handled under BSL-2 conditions according to Institutional Animal Care and Use Committee (IACUC)-approved protocols.

Cell lines and culture

The murine colon adenocarcinoma cells MC38 (Kerafast) and CT26 (ATCC) and Lewis lung carcinoma line (designated LLC) (Millipore Sigma) were maintained in complete media containing RPMI 1640 (Cytiva) supplemented with 10% heat-inactivated FBS (Corning), Penicillin/Streptomycin/Amphotericin B, 2 mM L-glutamine, 1 mM sodium pyruvate, and MEM non-essential amino acids (all from Thermo Fisher) at 37°C with 5% CO₂. Tumor cell lines were deficient in RGS5 expression (Supplementary Figure S1 and data not shown) and routinely confirmed to be mycoplasma-free prior to *in vitro* or *in vivo* studies.

Lm-based vaccines

Lm-based vaccines were engineered using a modified pGG-34 plasmid to include truncated listeriolysin O alone (designated Lm-LLO) or LLO fused to full-length murine RGS5 (NCBI Reference Sequence: NM_009063.5) (designated Lm-LLO-RGS5). LLO serves to facilitate intracellular infection as well as increase the immunogenicity of conjugated proteins.²⁴ A Mage-b Lm-based vaccine (a kind gift from Dr. Claudia Gravekamp, Albert Einstein College of Medicine) was incorporated as an internal control for immune reactivity against tumor cells *in vivo*.²⁵ All engineered constructs also contained a c-terminal Myc-tag to enable convenient protein detection in downstream assays. The attenuated Lm strain XFL-7 was electroporated with plasmids and streaked on brain heart infusion (BHI) plates (Bacto™, Thermo Fisher) under streptomycin/chloramphenicol selection as previously described.²⁶ Briefly, individual colonies were inoculated in 5 mL BHI (with streptomycin/chloramphenicol) and cultured overnight under shaking conditions at 37°C. Lm vaccine stocks were then established by seeding fresh BHI with Lm starter cultures at a 1:200 dilution, incubated at 37°C with shaking until OD600 measurements reached 0.6–0.8, and frozen at –80°C for up to 3 months. Prior to use in animals, titers of frozen Lm vaccine stocks were determined by colony-forming units (CFU) as documented.²⁷

Western blotting

To validate the protein-secreting capability of listeria-based vaccines, a 25 mL BHI culture was inoculated with a 1:100 dilution of a relevant Lm starter culture, and incubated with shaking at 37°C for 6 hr. The culture was then centrifuged at

10,000 × g for 5 min at 4°C, and cell-free supernatant passed through a 10 MWCO centrifugal filter (Amicon, MilliporeSigma) until sufficiently concentrated. Samples were diluted in beta-mercaptoethanol-containing Laemmli SDS buffer (Bio-Rad), boiled, and resolved on a 4–15% gradient Bis-Tris gel through SDS-PAGE. Proteins were next transferred to a PVDF membrane, blocked with 2.5% nonfat dry milk for one hour at room temperature, and incubated with a primary anti-Myc antibody (clone 9E10) (Biolegend) overnight at 4°C. Blots were washed with 0.5% Tween 20 in PBS (PBST), and probed with a goat anti-mouse IgG-HRP reagent (#A16072, Thermo Fisher) for 1 hr at room temperature. Following additional wash steps, blots were developed using SignalFire ECL (Cell Signaling Technology) and imaged on a Bio-Rad ChemiDoc Touch imaging System.

Tumor challenge model

Mice were randomly assigned to treatment groups (containing 5 mice/cohort) and received weekly escalating doses of Lm-based vaccines (1 × 10⁷ CFU, 5 × 10⁷ CFU, then 1 × 10⁸ CFU) by intraperitoneal (i.p.) injection in a total volume of 100 μL PBS as depicted in Figure 2a. Ten days following the initial vaccination, animals were subcutaneously (s.c.) challenged with 5 × 10⁵ tumor cells. ICB was also incorporated with i.p. injections of 100 μg of PD-1 blocking antibody (clone RMP1-14) (Bio X Cell) on days 1, 6, and 11 in all mice regardless of treatment cohort. Tumor sizes and animal weights were obtained every 2–3 days in a single-blind fashion. Overall longitudinal tumor volumes were determined using digital Vernier calipers and the formula (a × b²) ÷ 2, where b represents the smallest of two tumor diameter measurements. At the conclusion of the study, animals were euthanized and tumors excised, weighed, and processed for further analysis.

DC vaccine generation and treatment

In select experiments, bone-marrow-derived mononuclear cells were collected from femurs and tibias of mice as previously described²⁸ and cultured in complete RPMI with murine IL-4 (5 ng/mL) (Peprotech) and GM-CSF (10 ng/mL) (Peprotech) for 5 days at 37°C with 5% CO₂. All cells were then collected, washed, and subjected to magnetic bead positive selection in order to isolate CD11c+ immature DCs according to the manufacturer's guidelines (Miltenyi Biotec). DCs were subsequently matured in fresh complete media for 24 hr containing the following α-Type-1-polarizing murine agents (all from Miltenyi Biotec unless otherwise stated):²⁹ 10 ng/mL IFN-α, 1 × 10³ IU/mL IFN-γ, 5 ng/mL TNF-α, 25 ng/mL IL-1-β, and 10 μg/mL poly (I:C) (Sigma). The following day, non-adherent cells were collected, pelleted, and resuspended in IMDM (Thermo Fisher) at 1 × 10⁶ cells/mL. Individual peptides (OVA_{257–264} [SIINFEKL], RGS5_{73–82} [YGFASFKSFL], or RGS5_{159–167} [YALMEKDSL] [Genscript]) were added to cells at a final concentration of 10 μg/mL and cultured at 37°C with 5% CO₂ for 3 hr. Peptide-loaded DCs were then

administered to mice bearing established MC38 s.c. tumors (on days 4 and 11 post tumor implantation) and supplemented with anti-PD1 on days 7, 10, and 13 (Supplementary Figure S2a).

Ex vivo CD8+ T cell analysis

Splenocytes were collected from vaccinated or vaccinated/tumor-treated mice and CD8+ T cells purified through magnetic bead positive selection (Miltenyi Biotec). CD8+ T cells were then cultured for 24 hr in the presence of plate-bound anti-CD28 antibody (clone 37.51) (Bio X Cell), washed, and exposed to MC38 tumor cells at a 10:1 E:T ratio in complete media at 37°C with 5% CO₂. Positive control wells were stimulated with 2 µg/mL ConA. After 48 hr, cell-free supernatants were collected and relative levels of IFN-gamma determined by ELISA (BD Biosciences). Raw O.D. values were standardized to their respective ConA-stimulated treatments and data expressed as a function of normalized absorbance at 450 nm.

Immunohistochemistry (IHC)

Harvested tissues were fixed with 10% neutral buffered formalin (Thermo Fisher) for 24 hr and then incorporated into paraffin blocks using an automated tissue processor (Leica TP1020). Blocks were cut into 5 µm sections and mounted on charged slides (Fisherbrand). Sections were washed in distinct stages with xylene and ethanol, and antigen retrieval performed by exposing slides to boiling 10 mM sodium citrate for 15 min. Cooled sections were incubated in 3% H₂O₂, washed in PBS, and blocked using 2.5% heat-inactivated horse serum (Thermo Fisher). Primary antibody incubation was performed overnight at 4°C in a humidified chamber with an anti-CD3 mAb (1:100 dilution; clone SP7) (Thermo Fisher) or anti-CD31 mAb (1:50 dilution; clone SP38) (Thermo Fisher). Sections were washed with PBST and an anti-Rabbit IgG-HRP reagent (Vector Laboratories) applied for 30 min at room temperature in the dark, followed by additional washes in PBST. Staining was developed using a Metal-Enhanced DAB Substrate kit (Thermo Fisher) according to the manufacturer's recommendations until appropriate color change was observed. Sections were finally counterstained with a 1:3 dilution of Hematoxylin 2 (Thermo Fisher) for 20 seconds, followed by washes with water, ethanol, and xylene before mounting in Acrymount (StatLab). Slides were imaged under bright field microscopy (Leica) and analyzed using Aperio ImageScope software (version 12.3.3.5048).

Immunofluorescence (IF)

Excised tumors were embedded in O.C.T. (Thermo Fisher) and snap frozen over dry ice. Ten-micron tissue sections were adhered to charged slides, fixed in 4% paraformaldehyde (Electron Microscopy Sciences), permeabilized with 0.2% Triton X-100 + 0.2 mM glycine (Fisher Scientific), and blocked with 5% FBS in 0.2% Triton X-100. Sections were then incubated with primary antibodies against CD31 (clone MEC 13.3) (BD Biosciences), PDGFR-β (clone G.290.3) (Thermo Fisher), and CD8 (clone 208) (Thermo Scientific) followed by donkey anti-rat 488 and donkey anti-rabbit 594 secondary antibodies (both from Jackson ImmunoResearch). Coverslips were

applied over an anti-fade mounting medium containing DAPI (Vector Laboratories) and processed for IF microscopy using a MICA Microhub microscope (Leica). Quantification of CD8 and CD31 staining was accomplished using the Leica Application Suite X software (version 1.4.4.26810).

Quantitative PCR (qPCR)

Relevant tissues were first processed in TRIzol (Thermo Fisher) and total RNA isolated using the DirectZol RNA Miniprep Kit (Zymo Research). cDNA was subsequently generated with the SuperScript IV First-Strand Synthesis System (Thermo Fisher). Various gene targets were amplified (with validated qPCR primers [Origene] [Supplementary Table S1]) and quantitated using a Fast SYBR Green Master Mix (Applied Biosystems) on a StepOnePlus real-time PCR thermocycler (Applied Biosystems). Specific amplicons were further verified by melt curve analysis. All qPCR reactions were performed in duplicate in a 96-well PCR plate (Bio-Rad) using the following cycling conditions: initial denaturation at 95°C for 20 min followed by 35 cycles at 95°C for 3 min and 60°C for 30 min. Finally, gene expression levels were normalized to GAPDH or beta-actin and relative fold changes determined using the 2^{-ΔΔCt} method.³⁰

Flow cytometry

Harvested specimens were minced and enzymatically digested in an HBSS-based solution containing type IV collagenase, type IV DNase, and type V hyaluronidase (all from MilliporeSigma) for 15 min at 37°C. Preparations were spiked with FBS to inactivate enzymes, passed through a 70 µm strainer to obtain single cells, and red blood cells lysed with a 5 min exposure to ACK buffer.

Cells were then separated into 96-well plates for various staining protocols. Non-stimulated cells were surface stained with combinations of the following antibodies (all reagents from Bio-Legend and diluted/used per the manufacturer's guidelines unless indicated otherwise): APC/Cy7-CD45 (clone 30-F11), PerCP/Cy5.5-CD4 (clone RM4-5), PE/Cy7-CD8 (clone 53-6.7), and Brilliant Violet 605-CD279 (PD-1) (clone 29F.1A12). Stimulated cells were incubated with a Cell Activation Cocktail Kit at 37°C with 5% CO₂ in complete media for 6 hours. Following wash steps with PBS, cells were stained with combinations of the following antibodies: APC/Cy7-CD45, PerCP/Cy5.5-CD4, PE/Cy7-CD8, APC-IL-2 (clone JES6-5H4), PE-IFN-gamma (clone XMG1.2) and FITC-TNF-alpha (clone MP6-XT22). All cells were exposed to the Zombie Aqua viability dye prior to flow cytometric analysis using a BD LSR Fortessa (BD Biosciences) and FlowJo™ v 10.8.1 software (BD Life Sciences). UltraComp eBeads (Thermo Fisher) were used to prepare single-color compensation controls for all fluorescently labeled antibodies. Fluorescence minus one (FMO) and isotype controls were also prepared for each panel in a similar manner to the specific staining detailed above. See Supplementary Figure S3 for specific gating strategies.

Statistical analysis

Select results were analyzed with either unpaired t-test or one-way ANOVA + post-hoc pairwise comparisons using

GraphPad Prism (version 9.3.1). Experiments analyzing tumor burden *in vivo* were performed using linear mixed effects regression models with random intercepts, making use of measured data across all time points. A Toeplitz covariance matrix was selected based on Bayesian information criterion for the model. To control the false positive rate in post-hoc analyses, *P* values were adjusted for multiple comparisons with Dunnett's test using SAS 9.4 4 (SAS Institute, Inc.). Mean differences with a *P* value < .05 were considered statistically significant. Data presented are representative of at least 3 independent experiments.

Results

Successful development and characterization of a *listeria*-based vaccine against RGS5

We sought to devise a pre-clinical colon cancer model that incorporates vaccination against murine-derived RGS5, which is naturally processed and presented by the endogenous MHC system. Initially, as a proof-of concept, MHC class I-presented RGS5 peptides were predicted by NetMHC 4.0,^{31,32} synthesized, and incorporated into bone marrow-derived matured DCs matured with an alpha Type-1 polarizing cytokine cocktail.^{29,33} Animals were challenged with RGS5^{null} MC38 tumor cells (Supplementary Figure S1) on day 0 and vaccinated with RGS5 or control peptide-pulsed DCs on days 4 and 11 (Supplementary Figure S2A). Longitudinal tumor sizing confirmed trends in improved tumor protection in mice mediating RGS5-specific immunity (Supplementary Figure S2B), indicating the potential utility of this immunotherapeutic approach. Yet, despite this demonstration of general anti-tumor effects, we elected to further our studies by utilizing an RGS5-encoded *Lm*-based vaccine that provides the following conceptual advantages: [i] *Lm* instills potent adjuvant effects and selectively infects myeloid cells such as DCs that naturally process and present distinct RGS5 peptides³⁴ and [ii] a vaccine incorporating various RGS5-presented peptides may help improve protection by instituting epitope spreading against other TME components³⁵. From a translational perspective, *Lm*-based strategies would also not require personalized patient inoculums.

Therefore, the *Lm*-relevant plasmid, pGG-34,³⁶ was first modified to encode transgenes for truncated LLO (tLLO) alone or fused to full-length murine RGS5 followed by a c-terminal Myc-tag (Figure 1a). The XFL-7 *Lm* strain was then electroporated with either modified pGG-34 plasmid, pGG34-LLO or pGG34-LLO-RGS5, and secreted proteins assessed by western blot based on anti-Myc reactivity. As indicated in Figure 1b, band sizes obtained from the electroporated *Lm* cultures corresponded to predicted molecular weights for tLLO (~60 kDa) or tLLO-RGS5 (~70 kDa). As an internal control, *Lm* without pGG-34 did not yield a visible protein product. These data demonstrate the integrity of our *Lm*-based vaccines and the ability of these vectors to induce secretion of encoded proteins in *Lm*.

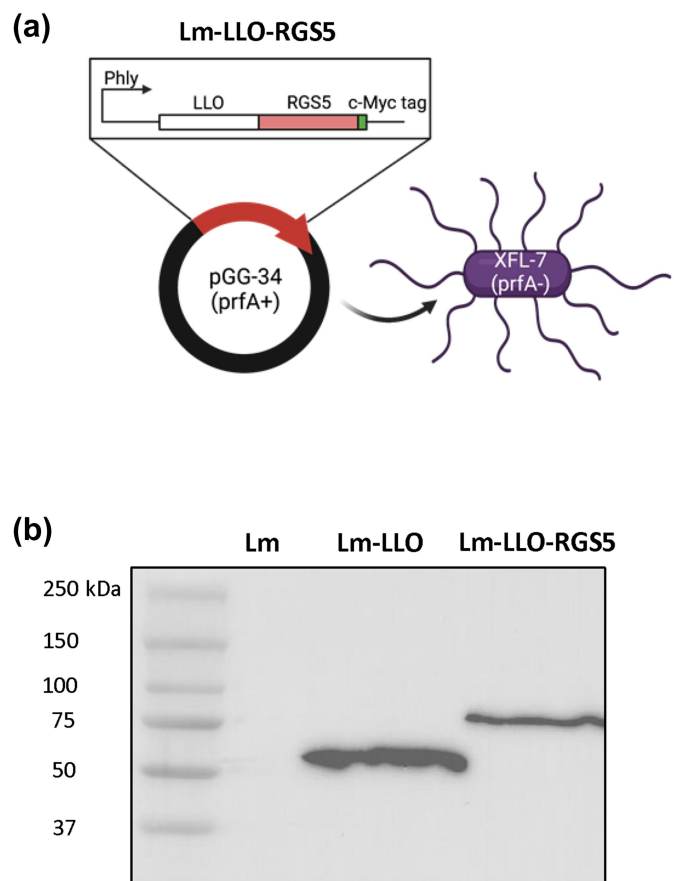


Figure 1. Construction and characterization of *Lm* vaccine strains. (a) The pGG-34 plasmid introduces truncated LLO into the attenuated, *prfA*-negative XFL-7 strain of *Lm*. LLO expression is controlled by the listerial hemolysin promoter (*phly*) and the potent transcription factor *prfA*. These gene-engineering strategies result in an immunogenic and attenuated strain of *Lm* capable of inducing a potent immune response without severe risk of listeriosis. (b) *Lm*-secreted LLO and LLO-RGS5 fusion proteins were detected by western blotting with an anti-Myc antibody. Abbreviations used: *Lm*, *Listeria monocytogenes*; LLO, listeriolysin O.

RGS5 vaccination safely enhances tumor protection in a murine model of colon cancer

As outlined in Figure 2a, C57BL/6 mice were challenged with MC38 tumor cells in tandem with increasing CFU doses of *Lm*-LLO or *Lm*-LLO-RGS5 (1×10^7 to 1×10^8 CFU) to safely induce immune activation, as similarly reported by others.^{10,25,37} PD-1 blockade was also instituted in mice to counter MC38-inspired immunosuppression and sustain vaccine-elicited immunity. We previously identified that PD-1 inhibition alone provided no observable protection relative to untreated MC38-challenged mice (Supplementary Figure S4A). Although *Lm*-LLO vaccination did not appear to provide demonstrable enhancements against cancer progression, *Lm*-LLO-RGS5 led to significant reductions in tumor size with evidence of blunted tumor growth kinetics over time (Figure 2b). Resected tumors of euthanized mice (at day 17) further corroborated these findings by indicating a greater than 50% reduction in tumor mass in *Lm*-LLO-RGS5-vaccinated mice compared to PBS and *Lm*-LLO control cohorts (Figure 2c). Our *Lm*-LLO-RGS5 vaccine regimen also exhibited enhanced tumor protection under a purely therapeutic scenario (Supplementary Figure S4B). These data are

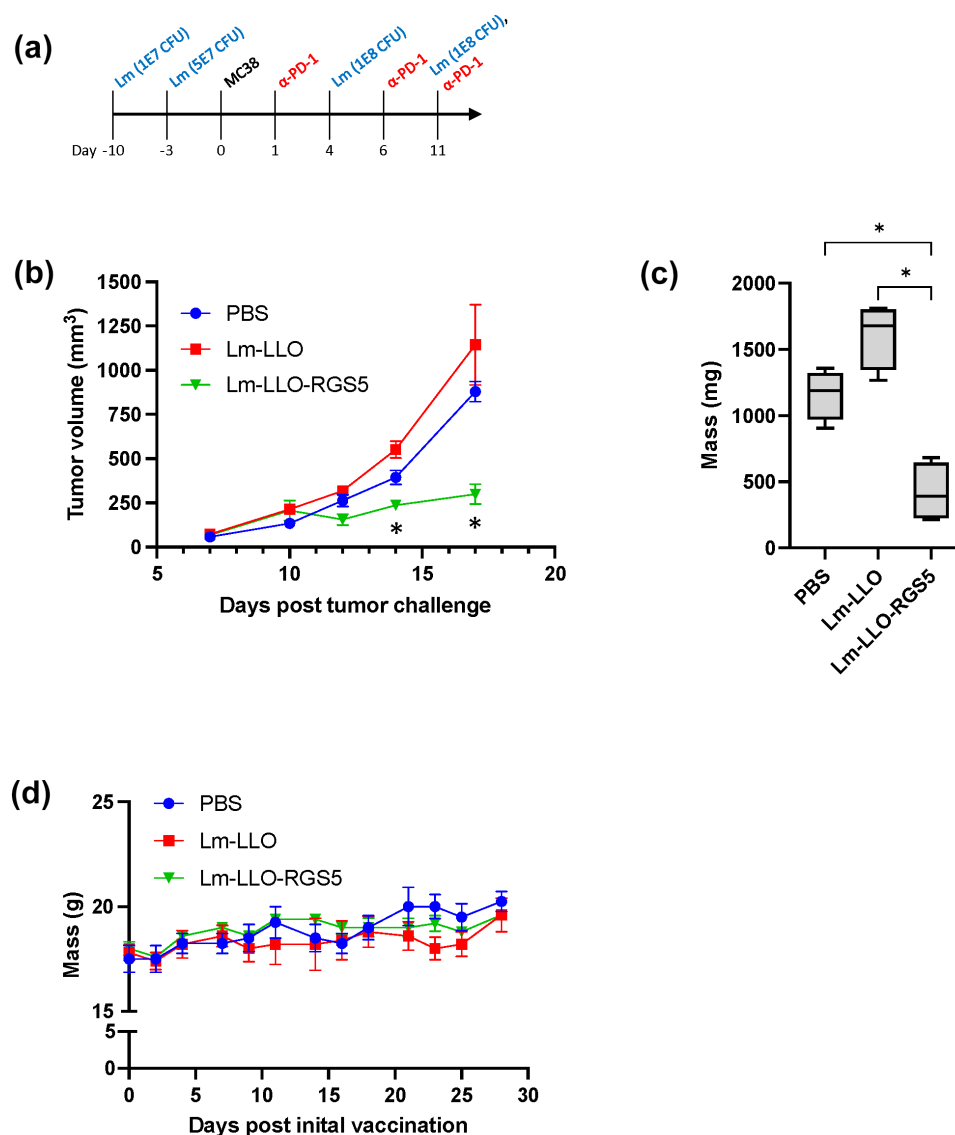


Figure 2. Lm-LLO-RGS5 treatment safely restricts MC38 tumor growth. (a) Schedule for tumor challenge, Lm-based vaccination, and ICB. (b) Longitudinal tumor growth curves and (c) associated tumor wet weights at study end. (d) Whole body weights of experimental mice post initial vaccination. * $P < .05$, bars \pm SEM. Abbreviations used: Lm, *Listeria monocytogenes*; LLO, listeriolysin O.

intriguing and require future study since, under this modeling scheme, animals did not receive the full complement of Lm-based vaccines given the constraints of the time course for Lm-based vaccine dose escalation and aggressiveness of the MC38 tumor model.

We assessed the safety of our Lm-based vaccines by analyzing mouse weights over time. Figure 2d indicates that our vaccine regimen did not adversely impact animal health based on minimal deviations from PBS animal weights (i.e., not exceeding 20% reduction in body mass). Additionally, heart, lung, and kidneys were harvested from euthanized mice at the conclusion of the study and examined by H&E. We were unable to find evidence that our Lm-based vaccines incited abnormal immune cell infiltration, tissue disturbance/destruction, or vascularity at these non-tumor sites (data not shown).

Overall, Lm-LLO-RGS5 vaccination safely provides animals improved control of MC38 growth *in vivo*. As MC38

cells do not endogenously express RGS5 (Supplementary Figure S1), immune-based activity is likely directed toward RGS5 expressing stromal content (such as pericytes) within the TME.

Immunizing against RGS5 directs cytotoxic T cells to colon cancer lesions

MC38 tumors were excised from euthanized mice at day 17 and examined by IHC for total CD3⁺ cells, presumed to mainly encompass T cells.³⁸ Although Lm-LLO vaccination demonstrated an increase in CD3⁺ cellular content, the most significant effects were observed in tumors from Lm-LLO-RGS5-treated mice (Figure 3a). More specifically, Lm-LLO-RGS5 vaccination induced a 2.7-fold increase in CD3⁺ cells compared to mice tolerated with Lm-LLO alone (614 [Lm-LLO-RGS5] vs. 224 [Lm-LLO] CD3⁺ cells per unit area).

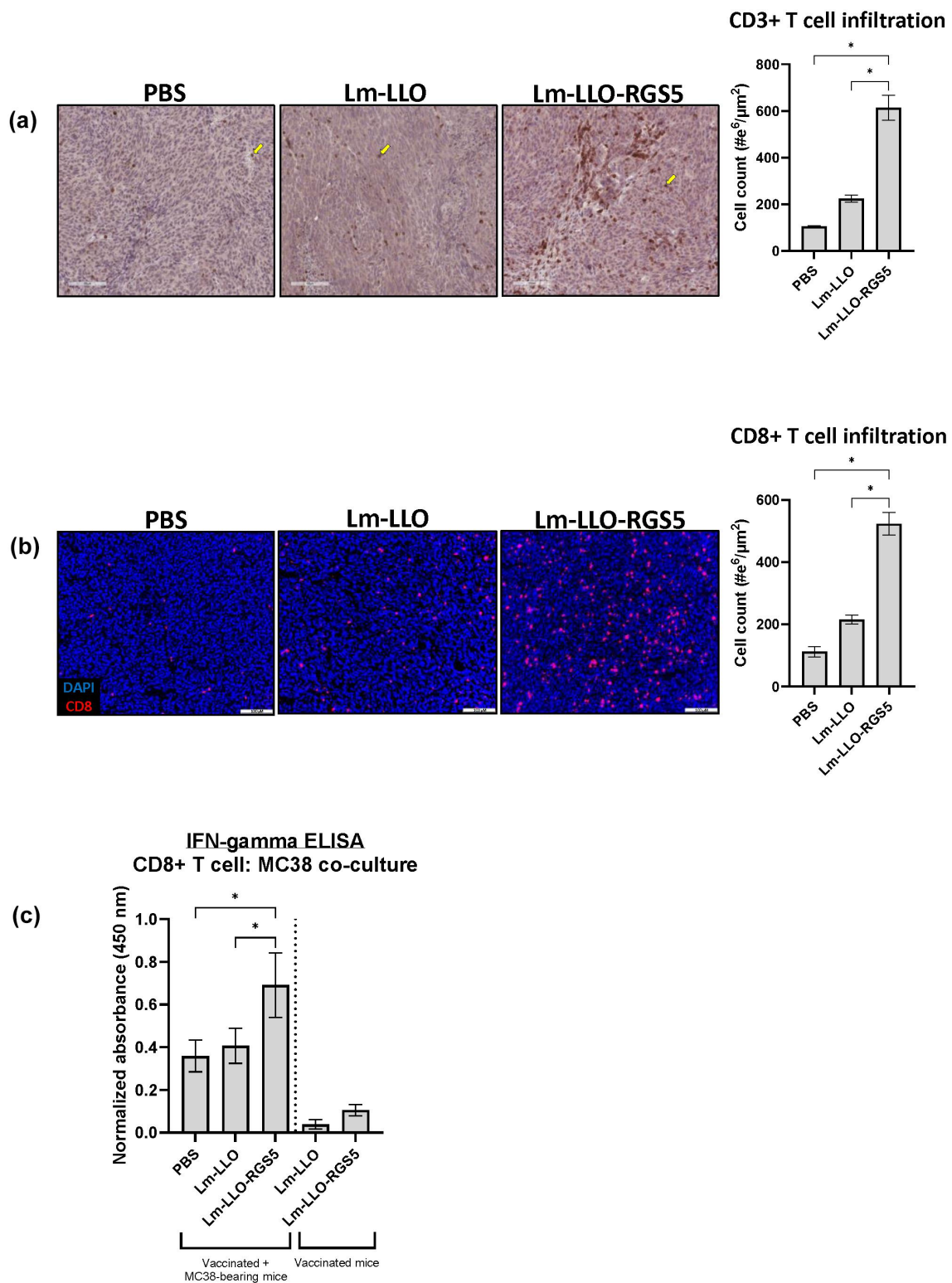


Figure 3. Lm-LLO-RGS5 immunization enhances effector T cell recruitment to MC38 tumors. (a) Representative CD3+ cell IHC staining in PBS, Lm-LLO, and Lm-LLO-RGS5-treated mice. 500 × 500-micron field views were randomly generated from tumors for each tumor lesion in an experimental group and total positive events averaged. (b) IF imaging for CD8+ T cells in PBS, Lm-LLO-treated, and Lm-LLO-RGS5-vaccinated animals. 650 × 550-micron fields were randomly selected from individual tumors in each experimental group and average counts obtained for each group. (c) CD8+ T cells were isolated from treated mice (Lm-based vaccine or Lm-based vaccine/MC38 tumor challenge) and co-cultured with MC38 tumor cells for 48 hr. IFN-gamma secretion was analyzed by ELISA and absorbance results normalized to ConA responses in control wells. **P* < .05, bars ± SEM. Yellow arrow inset demarking a stained cell of interest. Abbreviations used: IF, immunofluorescence; IHC, immunohistochemistry; Lm, *Listeria monocytogenes*; LLO, listeriolysin O.

These data were validated more specifically by IF in Figure 3b, indicating a greater than 2-fold increase of CD8+ T cells in tumors following Lm-LLO-RGS5 treatment (523 [Lm-LLO-RGS5] vs. 215 [Lm-LLO] CD8+ T cells per unit area). Considering the potential protective role of CD8+ T cells in our model, CD8+ T cells were isolated from spleens of treated animals to determine tumor antigen specificity. As MC38 do not express RGS5, Lm-LLO-RGS5 immunization alone did not afford reactivity against the tumor cell line *ex vivo* using CD8+ T cell secretion of IFN-gamma as a surrogate marker for T cell cytotoxicity (Figure 3c).^{39,40} However, in cases where tumor-bearing animals were vaccinated with Lm-LLO-RGS5, reactivity against MC38 cells was readily evident (versus other treatment cohorts). These results help establish that an initial RGS5-based immune response provokes epitope spreading against other TAAs.

We next analyzed T cell subsets in MC38 tumor lesions in greater detail through flow cytometry. Altogether, Lm-LLO-RGS5 vaccination resulted in significantly heightened frequencies of tumor-derived CD4+ (6.4% [Lm-LLO-RGS5] vs. 2.9% [Lm-LLO]) and CD8+ (12.9% [Lm-LLO-RGS5] vs. 5.4% [Lm-LLO]) T cells (Figure 4a). Such dynamics were not found systemically where circulating CD4+ and CD8+ T cell frequencies appeared equivalent between treatment groups (Supplementary Figure S5). More tumor-confined lymphocytes also maintained PD-1 positivity post RGS5 vaccination (CD4+ T cells at 3.6% [Lm-LLO-RGS5] vs. 1.0% [Lm-LLO]; CD8+ T cells at 6.2% [Lm-LLO-RGS5] vs. 2.1% [Lm-LLO]), again, suggesting a cytotoxic T cell phenotype (Figure 4b).⁴¹ Additionally, RGS5-inspired CD4+ and CD8+ T cells isolated from tumor lesions and stimulated *ex vivo* displayed significantly raised expression of IL-2 (CD4+ T cells at 4.6% [Lm-LLO-RGS5] vs. 2.5% [Lm-LLO]; CD8+ T cells at 4.9% [Lm-LLO-RGS5] vs. 2.5% [Lm-LLO]) (Figure 4c), IFN-gamma (CD4+ T cells at 5.4% [Lm-LLO-RGS5] vs. 2.0% [Lm-LLO]; CD8+ T cells at 24.7% [Lm-LLO-RGS5] vs. 8.9% [Lm-LLO]) (Figure 4d), and TNF-alpha (CD4+ T cells at 8.4% [Lm-LLO-RGS5] vs. 5.3% [Lm-LLO]; CD8+ T cells at 22.0% [Lm-LLO-RGS5] vs. 7.5% [Lm-LLO]) (Figure 4e). Lastly, qPCR of whole tumor tissues further confirmed our flow cytometry results, suggesting infiltrating lymphocytes established a Type-1 immune response in the TME since relative mRNA levels of IL-2, IFN-gamma, TNF-alpha, and PD-1 were also significantly elevated in Lm-LLO-RGS5 vaccinated mice (Figure 4f). With specific regard to TNF-alpha, the cytokine has pro- or anti-tumor characteristics in certain situations.⁴² Although we are utilizing the cytokine as an inflammatory marker for Type-1-mediated responses, elevated TNF-alpha expression in the TME correlated to improved tumor protection under our pre-clinical modeling, which is unsurprising given similar properties with other Lm-based anti-cancer vaccination strategies.⁴³ Future transcriptional profiling will also help resolve dominant T cell profiles and TCR clonotypes in the TME, but these data help support that Lm-LLO-RGS5 immunization drives antigen-specific and Type-1-associated T cells into tumors, which likely help instigate MC38 control.

Colon cancer vascularization is impaired following RGS5 vaccination

Previous studies have documented the anti-angiogenic effects of blood vessel-specific immunotherapies (incorporating RGS5 targeting), which account for tumor regression and protection *in vivo*.²¹ In our own unique pre-clinical system, vascular networks within the MC38 TME of RGS5 immunized mice were severely diminished. Lm-LLO-RGS5 vaccination led to significant reductions of intra-tumoral CD31+ vessels based on assessments by IHC (24 [Lm-LLO-RGS5] vs. 34 [Lm-LLO] CD31+ vessels per unit area) (Figure 5a) and IF (225 [Lm-LLO-RGS5] vs. 521 [Lm-LLO] CD31+ vessels per unit area) (Figure 5b). These measurements were corroborated by qPCR demonstrating significant losses of vascular markers associated with pericytes (RGS5, PDGFR-beta, and NG2) (Figure 5c) and endothelial cells (CD31 and VEGFR2) in tumor tissues relative to PBS or Lm-LLO treatment (Figure 5d). Yet, these drastic vasculature effects did not appear to simply be a function of smaller tumor size due to immune-based control. To test this possibility, we incorporated a separate Lm-based vaccine targeting Mage-b (directly expressed by MC38 cells [Supplementary Figure S1A]) in keeping with the treatment schedule outlined in Figure 2a. Although tumor protection was readily apparent (compared to Lm-LLO treatment) based on immune-mediated specificity against tumor cells (Supplementary Figure S6A), relative tumor vascularity was maintained between treatment groups when assessing tumor tissues for CD31+ cells by IHC and qPCR (Supplementary Figure S6B).

The Lm-LLO-RGS5 vaccine's anti-vascular effects were also confirmed against other relevant *in vivo* tumor models. First, BALB/c mice were vaccinated and s.c. challenged with the CRC cell line CT26⁴⁴ alongside ICB treatment as detailed in Figure 2a. Similar to MC38, CT26 expresses PD-L1 that plays a critical role in suppressing anti-tumor T cell responses.⁴⁵ IHC was performed on terminally resected CT26 tumors and significant reductions in intra-tumoral CD31+ blood vessel density were demonstrated as detailed in Figure 6a. Such effects were, likewise, verified through qPCR based on relative fold reductions in the expression of endothelial cell (CD31) and pericyte (RGS5) markers in the TME (Figure 6a). Additionally, to better gauge the broad applicability of the Lm-LLO-RGS5 treatment regimen (given our focus on a conserved vascular target), C57BL/6 mice were treated and s.c. inoculated with the LLC cell line (Figure 2a). LLC cells are characterized as poorly immunogenic based on the down-regulation of immune-related gene signatures that include MHC class I⁴⁴ and culminate in resistance to ICB.^{44,46} Intriguingly, Lm-LLO-RGS5 vaccination resulted in reduced LLC-derived vascularity when assessed by IHC and qPCR (Figure 6b).

In summary, our studies provide supportive evidence that an Lm-LLO-RGS5 vaccine safely instills and directs cytotoxic T cells to the TME, and improved cancer protection is partly achieved by immune-mediated activity against tumor-derived blood vessels.

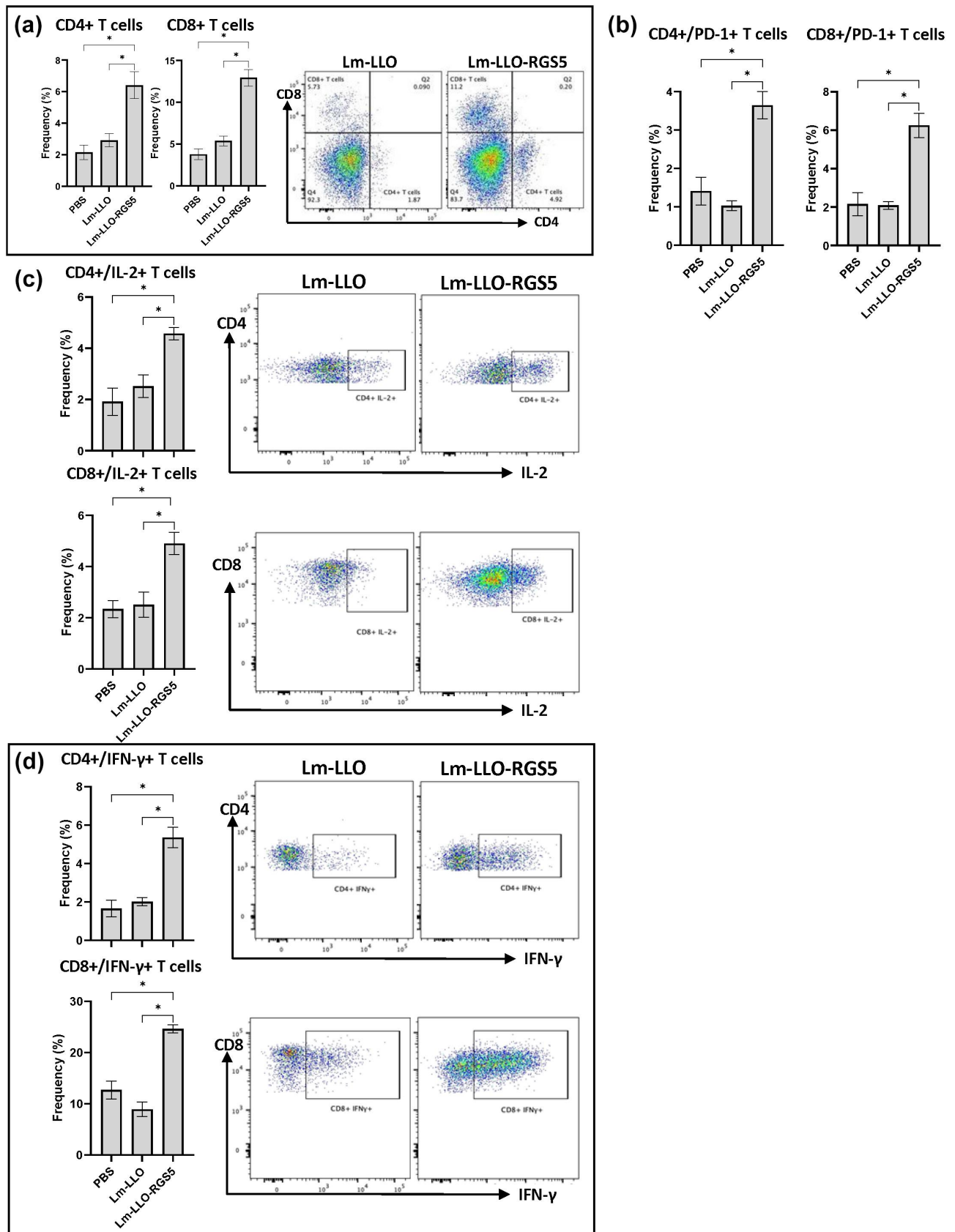


Figure 4. Lm-LLO-RGS5 vaccination generates type-I skewed CD4+ and CD8+ T cells. Single-cell suspensions from tumors were prepared, stained, gated, and analyzed for flow cytometry as described in the Materials and Methods section. Frequencies of live (a) CD4+/CD8+ T cells, (b) PD-1+ T cells, (c) IL-2+ T cells, (d) IFN-gamma+ T cells, and (e) TNF-alpha+ T cells are reported alongside representative scatter plots. (f) qPCR analysis of genes associated with cytotoxic CD8+ T cells within MC38 tumors. Gene expression was normalized to a housekeeping gene and presented as relative fold-change. * $P < .05$, bars \pm SEM. Abbreviations used: Lm, *Listeria monocytogenes*; LLO, listeriolysin O; qPCR, quantitative PCR; TME, tumor microenvironment.

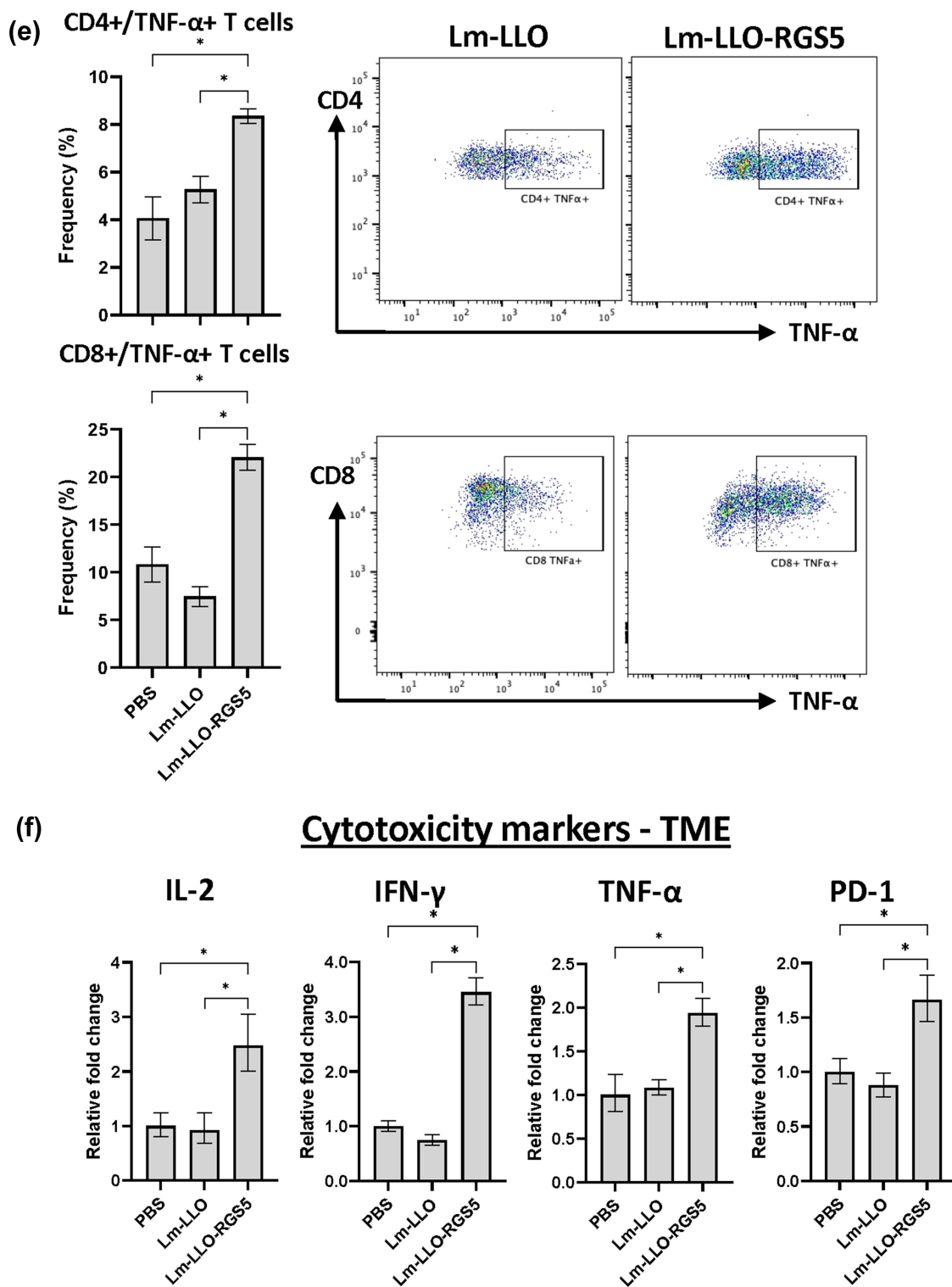


Figure 4. Continue

Discussion

Despite FDA-approved ICB and anti-angiogenic strategies to treat mCRC, the short-term successes of these options have not converted to durable objective responses for patients. CRC presents as a highly immunosuppressive TME that can rapidly develop ICB resistance while delivering several immune-related adverse effects.⁴⁷ A potentially improved approach

that is applicable to most patients involves engaging effector T cells to destroy blood vessel content within the TME, which serves to abrogate cancer progression and establish “normal” blood flow dynamics that reinforce the distribution and function of Type-1-associated immune cells.^{48,49} Indeed, immunotherapeutic strategies against TBVAs are generally safe in patients and have shown therapeutic promise in early-phase

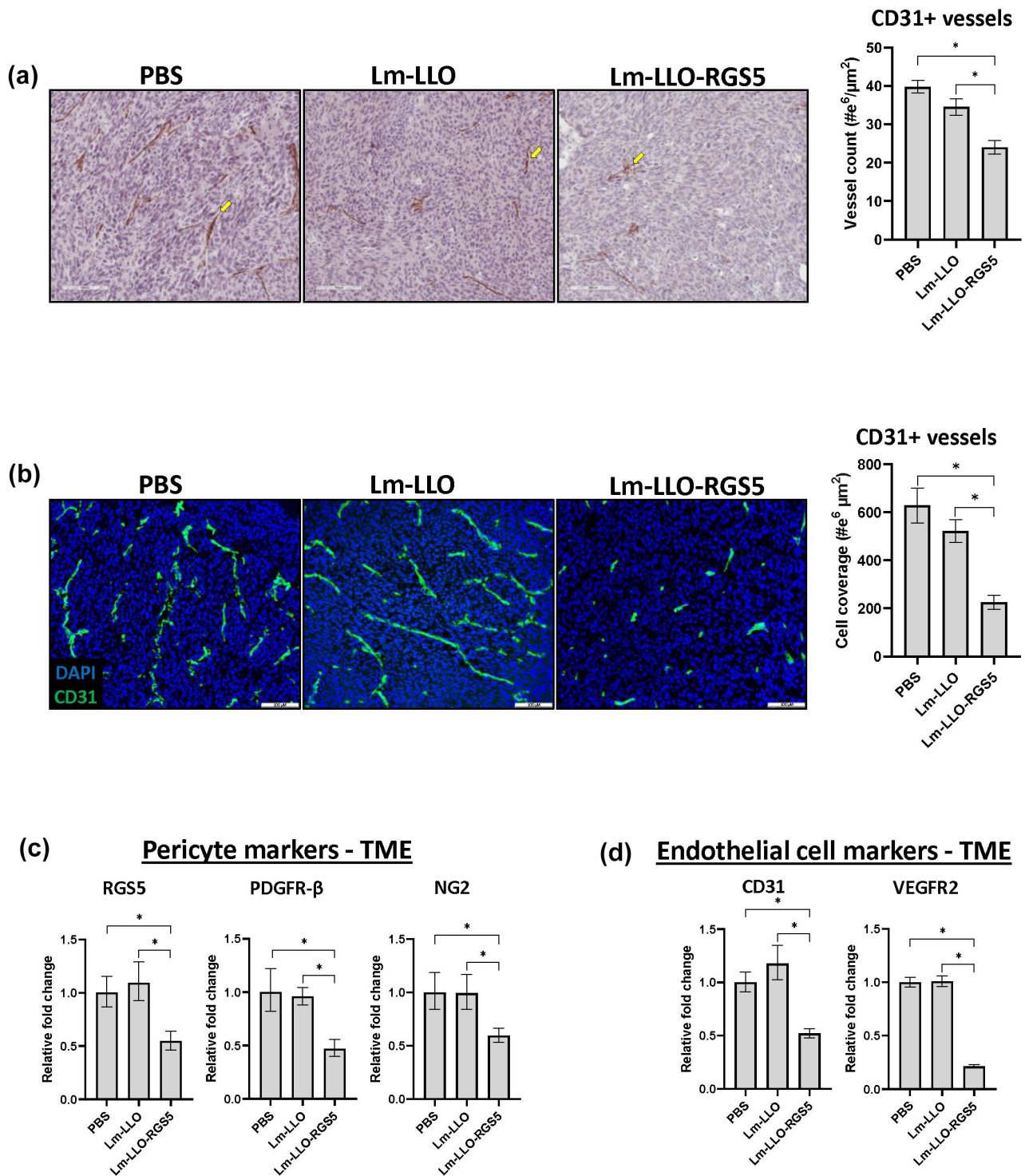


Figure 5. Lm-LLO-RGS5 treatment restricts MC38 tumor vascularity. (a) Representative IHC images of CD31+ cells for PBS, Lm-LLO, and Lm-LLO-RGS5-vaccinated mice. 500 × 500-micron fields were randomly generated and quantitated to generate average counts per treatment. (b) IF demonstration of CD31+ cells across PBS and Lm-LLO- and Lm-LLO-RGS5 treatments. 650 × 550-micron fields were randomly selected for individual tumors and qPCR analysis of genes associated with (c) pericytes and (d) endothelial cells within MC38 tumors and total positive events averaged. Gene expression was normalized relative to a housekeeping gene and reported as relative fold-change. **P* < .05, bars ± SEM. Yellow arrow inset distinguishing a stained cell of interest. Abbreviations used: IF, immunofluorescence; IHC, immunohistochemistry; Lm, *Listeria monocytogenes*; LLO, listeriolysin O; qPCR, quantitative PCR; TME, tumor microenvironment.

clinical trial evaluations.^{50–52} Pericytes, in particular, represent an ideal vascular target given their role in facilitating sprouting angiogenesis and stabilizing endothelial tubes in the TME.^{53,54}

RGS5 is a critical intracellular mediator for signaling in pericytes, and, therefore, may represent an important depot

for MHC class I-presented peptides that elicit CD8⁺ T cell immunity. RGS5-targeted DC vaccines have previously been documented to reduce tumor burden in MC38 and B16 cell lines using HLA-A2 transgenic mice.²¹ Although this pre-clinical system predicted RGS5-specific immunity (against

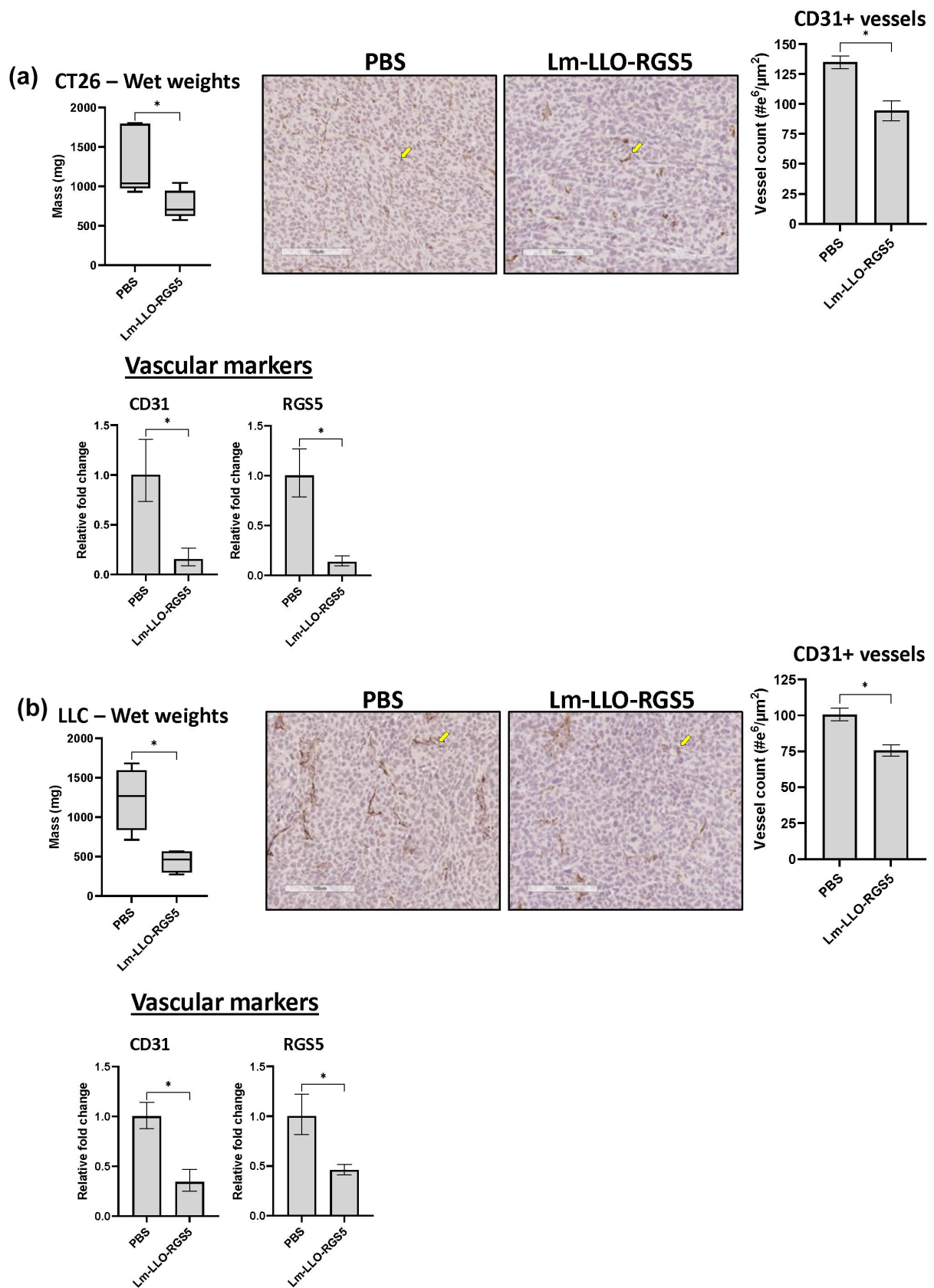


Figure 6. Lm-LLO-RGS5 vaccination elicits anti-vascular effects across cancer models. As detailed in Figure 5, tumor vascularity was assessed by IHC and qPCR for animals inoculated with either (a) CT26 or (b) LLC tumor lines. * $P < .05$, bars \pm SEM. Yellow arrow inset distinguishing a stained cell of interest. Abbreviations used: IHC, immunohistochemistry; Lm, *Listeria monocytogenes*; LLO, listeriolysin O; qPCR, quantitative PCR.

the HLA-A2 epitope LAALPHSCL) in 25% of individuals with melanoma,²³ the ability to more fully understand vaccine-inspired settings of cancer regression and/or progression against self-antigens like RGS5 are potentially limited by mouse modeling issues such as inconsistent HLA-A2 tissue expression and the artificial nature of inducing (seemingly moderate-to-high affinity) murine CD8+ T cells against HLA-A2-presented epitopes.^{55,56} The nature of our modeling/vaccine system reported here attempts to resolve such dilemmas by analyzing endogenous immune system responses against a self-TBVA that more conceptually recapitulates the patient experience. Ultimately, we utilized a Lm-based vaccine as a tool to facilitate DC processing/presentation of multiple RGS5-specific epitopes. These efforts did not require us to delineate immunogenic MHC-presented peptides for immunization purposes (although our preliminary vaccine efforts with DCs indicate these do exist [Supplementary Figure S2]). Our escalating Lm-LLO-RGS5 dose strategy generated a Type-1-associated immune response that safely promoted protection against RGS5^{null} colon cancer progression in mice. Our observed influx of intratumoral CD4+ and CD8+ T cells also correlated to significant losses in vascular density and TBVAs associated with pericytes and endothelial cells. We envision that initial CD8+ T cell-driven responses against targetable RGS5+ stromal cells following Lm-based vaccine treatment in the TME [i] drive epitope spreading against other TAAs (Figure 3c) and [ii] improve T cell infiltration through vessel “normalization,” considering that residual vessels in Lm-LLO-RGS5 vaccinated animals were associated with pericytes (Supplementary Figure S7). These findings would need to be confirmed and better understood in prospective studies though. Nevertheless, these results support a strategy of directing an initial immune response against RGS5+ stromal cells like pericytes under the setting of CRC to potentiate protection against established disease or in patients at high-risk of developing cancer (e.g., Lynch syndrome). Current work in our laboratory is now focused on more specifically interrogating immune-mediated actions against RGS5 in colon cancer experimentally established in the distal large intestine. However, given RGS5’s conserved expression and ability to inspire anti-tumor effects against various cancer types (Figure 6), this Lm-based vaccination regimen would likely apply to other vascularized malignancies.

From a translational standpoint, Lm-based vaccines could represent an option for patients. Currently, Lm-based vaccines have been in development for over two decades with significant clinical trial experience.¹³ Early phase I efforts demonstrated promising safety profiles with either oral or intravenous administration routes.^{57,58} Lm-based vaccines have since proceeded through several patient trials for a number of different malignancies (e.g., HPV-associated cervical cancer, malignant pleural mesothelioma, canine osteosarcoma) and have continued to demonstrate favorable safety with promising efficacy.¹³ A recent phase 2 clinical trial completed in patients with advanced pancreatic cancer receiving an Lm-based vaccine targeting mesothelin also inferred improved survival⁵⁹. This strategy incorporated

cyclophosphamide/GVAX followed by Listeria-based vaccination + ICB and yielded long-term survivors with increased intratumoral CD8+ T cell frequencies and reduced immunosuppressive myeloid cells. Additional clinical efforts with Lm-based vaccines are ongoing with a human osteosarcoma trial following successful studies of an Lm-based vaccine targeting HER2 in canine osteosarcoma.⁶⁰ Ultimately, the ability of Lm-based vaccines to induce biological changes in the TME that are tied to patient prognosis⁶¹ support additional efforts to expand evaluations in larger cohorts of cancer patients.

Overall, our study provides an initial proof-of-principle for utilizing Lm-based vaccines against colon cancer-derived blood vessels. Improving basic knowledge surrounding immune system dynamics and potential combinational regimens will ultimately be important in helping inform future RGS5-based immunotherapies for individuals with CRC.

Acknowledgments

We thank Dr. Ulrich Bickel and Yeseul Ahn for technical assistance in helping establish IF staining, imaging, and analysis. DBL is supported in part by funds from the Cancer Prevention and Research Institute of Texas (CPRIT) (RP210154), NIH (R15 CA215874), DOD (W81XWH-18-1-0293), and Dodge Jones Foundation-Abilene. All included graphics were created with Biorender.com.

Disclosure statement

No potential conflict of interest was reported by the author(s).

Funding

The work was supported by the NIH [R15 CA215874,]; Dodge Jones Foundation-Abilene CPRIT [RP210154]; DoD [W81XWH-18-1-0293,].

Data availability statement

The data that support the findings of this study are available from the corresponding author (D.B.L.) upon reasonable request.

References

1. Xi Y, Xu P. Global colorectal cancer burden in 2020 and projections to 2040. *Transl Oncol.* 2021;14(10):101174. doi:10.1016/j.tranon.2021.101174.
2. Sung H, Ferlay J, Siegel RL, Laversanne M, Soerjomataram I, Jemal A, Bray F. Global cancer statistics 2020: GLOBOCAN estimates of incidence and mortality worldwide for 36 cancers in 185 countries. *CA Cancer J Clin.* 2021;71(3):209–249. doi:10.3322/caac.21660.
3. Turano M, Delrio P, Rega D, Cammarota F, Polverino A, Duraturo F, Izzo P, De Rosa M. Promising colorectal cancer biomarkers for precision prevention and therapy. *Cancers Basel.* 2019;11(12):1932. doi:10.3390/cancers11121932.
4. Van der Jeught K, Xu H-C, Li Y-J, Lu X-B, Ji G. Drug resistance and new therapies in colorectal cancer. *World J Gastroenterol.* 2018;24(34):3834–3848. doi:10.3748/wjg.v24.i34.3834.
5. Douillard JY, Cunningham D, Roth AD, Navarro M, James RD, Karasek P, Jandik P, Iveson T, Carmichael J, Alakl M, et al. Irinotecan combined with fluorouracil compared with fluorouracil alone as first-line treatment for metastatic colorectal cancer:

- a multicentre randomised trial. *Lancet*. 2000;355(9209):1041–1047. doi:10.1016/S0140-6736(00)02034-1.
6. Fan A, Wang B, Wang X, Nie Y, Fan D, Zhao X, Lu Y. Immunotherapy in colorectal cancer: current achievements and future perspective. *Int J Biol Sci*. 2021;17(14):3837–3849. doi:10.7150/ijbs.64077.
 7. Jia W, Zhang T, Huang H, Feng H, Wang S, Guo Z, Luo Z, Ji X, Cheng X, Zhao R, et al. Colorectal cancer vaccines: the current scenario and future prospects. *Front Immunol*. 2022;13:942235. doi:10.3389/fimmu.2022.942235.
 8. Berry J, Vreeland T, Trappey A, Hale D, Peace K, Tyler J, Walker A, Brown R, Herbert G, Yi F, et al. Cancer vaccines in colon and rectal cancer over the last decade: lessons learned and future directions. *Expert Rev Clin Immunol*. 2017;13(3):235–245. doi:10.1080/1744666X.2016.1226132.
 9. Sanchez-Leon ML, Jiménez-Cortegana C, Cabrera G, Vermeulen EM, de la Cruz-Merino L, Sánchez-Margalet V. The effects of dendritic cell-based vaccines in the tumor microenvironment: impact on myeloid-derived suppressor cells. *Front Immunol*. 2022;13:1050484. doi:10.3389/fimmu.2022.1050484.
 10. Jahangir A, Chandra D, Quispe-Tintaya W, Singh M, Selvanesan BC, Gravekamp C. Immunotherapy with *Listeria* reduces metastatic breast cancer in young and old mice through different mechanisms. *Oncoimmunology*. 2017;6(9):e1342025. doi:10.1080/2162402X.2017.1342025.
 11. Oladejo M, Nguyen H-M, Seah H, Datta A, Wood LM. Tumoral CD105 promotes immunosuppression, metastasis, and angiogenesis in renal cell carcinoma. *Cancer Immunol Immunother*. 2023;72(6):1633–1646. doi:10.1007/s00262-022-03356-5.
 12. Zhou S, Gravekamp C, Bermudes D, Liu K. Tumour-targeting bacteria engineered to fight cancer. *Nat Rev Cancer*. 2018;18(12):727–743. doi:10.1038/s41568-018-0070-z.
 13. Oladejo M, Paterson Y, Wood LM. Clinical experience and recent advances in the development of *Listeria*-based tumor immunotherapies. *Front Immunol*. 2021;12:642316. doi:10.3389/fimmu.2021.642316.
 14. Fabian KL, Storkus WJ. Immunotherapeutic targeting of tumor-associated blood vessels. *Adv Exp Med Biol*. 2017;1036:191–211.
 15. Schaaf MB, Garg AD, Agostinis P. Defining the role of the tumor vasculature in antitumor immunity and immunotherapy. *Cell Death Disease*. 2018;9(2):115. doi:10.1038/s41419-017-0061-0.
 16. Martin JD, Seano G, Jain RK. Normalizing function of tumor vessels: progress, opportunities, and challenges. *Annu Rev Physiol*. 2019;81(1):505–534. doi:10.1146/annurev-physiol-020518-114700.
 17. Garza Trevino EN, González PD, Valencia Salgado CI, Martínez Garza A. Effects of pericytes and colon cancer stem cells in the tumor microenvironment. *Cancer Cell Int*. 2019;19(1):173. doi:10.1186/s12935-019-0888-9.
 18. Berger M, Bergers G, Arnold B, Hammerling GJ, Ganss R. Regulator of G-protein signaling-5 induction in pericytes coincides with active vessel remodeling during neovascularization. *Blood*. 2005;105(3):1094–1101. doi:10.1182/blood-2004-06-2315.
 19. Dabravolski SA, Andreeva ER, Eremin II, Markin AM, Nadelyaeva II, Orekhov AN, Melnichenko AA. The role of pericytes in regulation of innate and adaptive immunity. *Biomedicines*. 2023;11(2):600. doi:10.3390/biomedicines11020600.
 20. Raza A, Franklin MJ, Dudek AZ. Pericytes and vessel maturation during tumor angiogenesis and metastasis. *Am J Hematol*. 2010;85(8):593–598. doi:10.1002/ajh.21745.
 21. Zhao X, Bose A, Komita H, Taylor JL, Chi N, Lowe DB, Okada H, Cao Y, Mukhopadhyay D, Cohen PA, et al. Vaccines targeting tumor blood vessel antigens promote CD8(+) T cell-dependent tumor eradication or dormancy in HLA-A2 transgenic mice. *J Immunol*. 2012;188(4):1782–1788. doi:10.4049/jimmunol.1101644.
 22. Hamzah J, Jugold M, Kiessling F, Rigby P, Manzur M, Marti HH, Rabie T, Kaden S, Gröne H-J, Hämmerling GJ, et al. Vascular normalization in Rgs5-deficient tumours promotes immune destruction. *Nature*. 2008;453(7193):410–414. doi:10.1038/nature06868.
 23. Storkus WJ, Maurer D, Lin Y, Ding F, Bose A, Lowe D, Rose A, DeMark M, Karapetyan L, Taylor JL, et al. Dendritic cell vaccines targeting tumor blood vessel antigens in combination with dasatinib induce therapeutic immune responses in patients with checkpoint-refractory advanced melanoma. *J Immunother Cancer*. 2021;9(11):e003675. doi:10.1136/jitc-2021-003675.
 24. Singh R, Dominiecki ME, Jaffee EM, Paterson Y. Fusion to listeriolysin O and delivery by *Listeria monocytogenes* enhances the immunogenicity of HER-2/neu and reveals subdominant epitopes in the FVB/N mouse. *J Immunol*. 2005;175(6):3663–3673. doi:10.4049/jimmunol.175.6.3663.
 25. Kim SH, Castro F, Gonzalez D, Maciag PC, Paterson Y, Gravekamp C. Mage-b vaccine delivered by recombinant *Listeria monocytogenes* is highly effective against breast cancer metastases. *Br J Cancer*. 2008;99(5):741–749. doi:10.1038/sj.bjc.6604526.
 26. Monk IR, Gahan CG, Hill C. Tools for functional postgenomic analysis of *Listeria monocytogenes*. *Appl Environ Microbiol*. 2008;74(13):3921–3934. doi:10.1128/AEM.00314-08.
 27. Jones GS, D’Orazio SEF. *Listeria monocytogenes*: cultivation and laboratory maintenance. *Curr Protoc Microbiol*. 2013;31(1):B9 2 1–B9 2 7. doi:10.1002/9780471729259.mc09b02s31.
 28. Son YI, Egawa S-I, Tatsumi T, Redlinger RE, Kalinski P, Kanto T. A novel bulk-culture method for generating mature dendritic cells from mouse bone marrow cells. *J Immunol Methods*. 2002;262(1–2):145–157. doi:10.1016/S0022-1759(02)00013-3.
 29. Mailliard RB, Wankowicz-Kalinska A, Cai Q, Wesa A, Hillkens CM, Kapsenberg ML, Kirkwood JM, Storkus WJ, Kalinski P. α -type-1 polarized dendritic cells. *Cancer Res*. 2004;64(17):5934–5937. doi:10.1158/0008-5472.CAN-04-1261.
 30. Livak KJ, Schmittgen TD. Analysis of relative gene expression data using real-time quantitative PCR and the 2⁻($\Delta\Delta C_T$) method. *Methods*. 2001;25(4):402–408. doi:10.1006/meth.2001.1262.
 31. Andreatta M, Nielsen M. Gapped sequence alignment using artificial neural networks: application to the MHC class I system. *Bioinformatics*. 2016;32(4):511–517. doi:10.1093/bioinformatics/btv639.
 32. Nielsen M, Lundegaard C, Worning P, Lauemøller SL, Lamberth K, Buus S, Brunak S, Lund O. Reliable prediction of T-cell epitopes using neural networks with novel sequence representations. *Protein Sci*. 2003;12(5):1007–1017. doi:10.1110/ps.0239403.
 33. Lowe DB, Bose A, Taylor JL, Tawbi H, Lin Y, Kirkwood JM, Storkus WJ. Dasatinib promotes the expansion of a therapeutically superior T-cell repertoire in response to dendritic cell vaccination against melanoma. *Oncoimmunology*. 2014;3(2):e27589. doi:10.4161/onci.27589.
 34. Liu Y, Niu L, Li N, Wang Y, Liu M, Su X, Bao X, Yin B, Shen S. Bacterial-mediated tumor therapy: old treatment in a New context. *Adv Sci*. 2023;10(12):e2205641. doi:10.1002/adv.202205641.
 35. Wood LM, Pan Z-K, Guirnalda P, Tsai P, Seavey M, Paterson Y. Targeting tumor vasculature with novel *Listeria*-based vaccines directed against CD105. *Cancer Immunol Immunother*. 2011;60(7):931–942. doi:10.1007/s00262-011-1002-x.
 36. Gunn GR, Zubair A, Peters C, Pan ZK, Wu TC, Paterson Y. Two *Listeria monocytogenes* vaccine vectors that express different molecular forms of human papilloma virus-16 (HPV-16) E7 induce qualitatively different T cell immunity that correlates with their ability to induce regression of established tumors immortalized by HPV-16. *J Immunol*. 2001;167(11):6471–6479. doi:10.4049/jimmunol.167.11.6471.
 37. Chandra D, Jahangir A, Quispe-Tintaya W, Einstein MH, Gravekamp C. Myeloid-derived suppressor cells have a central role in attenuated *Listeria monocytogenes*-based immunotherapy against metastatic breast cancer in young and old mice. *Br J Cancer*. 2013;108(11):2281–2290. doi:10.1038/bjc.2013.206.
 38. Kheirrolomoom A, Kare AJ, Ingham ES, Paulmurugan R, Robinson ER, Baikoghli M, Inayathullah M, Seo JW, Wang J, Fite BZ, et al. In situ T-cell transfection by anti-CD3-conjugated lipid nanoparticles leads to T-cell activation, migration, and

- phenotypic shift. *Biomaterials*. 2022;281:121339. doi:10.1016/j.biomaterials.2021.121339.
39. Ghanekar SA, Nomura LE, Suni MA, Picker LJ, Maecker HT, Maino VC. Gamma interferon expression in CD8+T cells is a marker for circulating cytotoxic T lymphocytes that recognize an HLA A2-restricted epitope of human cytomegalovirus phosphoprotein pp65. *Clin Diagn Lab Immunol*. 2001;8(3):628–631. doi:10.1128/CDLI.8.3.628-631.2001.
 40. Horton H, Russell N, Moore E, Frank I, Baydo R, Havenar-Daughton C, Lee D, Deers M, Hudgens M, Weinhold K, et al. Correlation between Interferon- γ secretion and cytotoxicity, in Virus-specific Memory T cells. *J Infect Dis*. 2004;190(9):1692–1696. doi:10.1086/424490.
 41. Simon S, Labarriere N. PD-1 expression on tumor-specific T cells: friend or foe for immunotherapy? *Oncoimmunology*. 2017;7(1):e1364828. doi:10.1080/2162402X.2017.1364828.
 42. Montfort A, Colacios C, Levade T, Andrieu-Abadie N, Meyer N, Ségui B. The TNF paradox in cancer progression and immunotherapy. *Front Immunol*. 2019;10:1818. doi:10.3389/fimmu.2019.01818.
 43. Oladejo M, Nguyen H-M, Silwal A, Reese B, Paulishak W, Markiewski MM, Wood LM. Listeria-based immunotherapy directed against CD105 exerts anti-angiogenic and anti-tumor efficacy in renal cell carcinoma. *Front Immunol*. 2022;13:1038807. doi:10.3389/fimmu.2022.1038807.
 44. Lechner MG, Karimi SS, Barry-Holson K, Angell TE, Murphy KA, Church CH, Ohlfest JR, Hu P, Epstein AL. Immunogenicity of murine solid tumor models as a defining feature of in vivo behavior and response to immunotherapy. *J Immunother* (1991). 2013;36(9):477–489. doi:10.1097/01.cji.0000436722.46675.4a.
 45. Lau J, Cheung J, Navarro A, Lianoglou S, Haley B, Totpal K, Sanders L, Koeppen H, Caplazi P, McBride J, et al. Tumour and host cell PD-L1 is required to mediate suppression of anti-tumour immunity in mice. *Nat Commun*. 2017;8(1):14572. doi:10.1038/ncomms14572.
 46. Li HY, McSharry M, Bullock B, Nguyen TT, Kwak J, Poczobutt JM, Sippel TR, Heasley LE, Weiser-Evans MC, Clambey ET, et al. The tumor microenvironment regulates sensitivity of murine lung tumors to PD-1/PD-L1 antibody blockade. *Cancer Immunol Res*. 2017;5(9):767–777. doi:10.1158/2326-6066.CIR-16-0365.
 47. Ganesh K, Stadler ZK, Cercek A, Mendelsohn RB, Shia J, Segal NH, Diaz LA. Immunotherapy in colorectal cancer: rationale, challenges and potential. *Nat Rev Gastroenterol Hepatol*. 2019;16(6):361–375. doi:10.1038/s41575-019-0126-x.
 48. Goel S, Duda DG, Xu L, Munn LL, Boucher Y, Fukumura D, Jain RK. Normalization of the vasculature for treatment of cancer and other diseases. *Physiol Rev*. 2011;91(3):1071–1121. doi:10.1152/physrev.00038.2010.
 49. Tian L, Goldstein A, Wang H, Ching Lo H, Sun Kim I, Welte T, Sheng K, Dobrolecki LE, Zhang X, Putluri N, et al. Mutual regulation of tumour vessel normalization and immunostimulatory reprogramming. *Nature*. 2017;544(7649):250–254. doi:10.1038/nature21724.
 50. Liu Z, Wang Y, Huang Y, Kim BYS, Shan H, Wu D, Jiang W. Tumor vasculatures: a New target for cancer immunotherapy. *Trends Pharmacol Sci*. 2019;40(9):613–623. doi:10.1016/j.tips.2019.07.001.
 51. Yang S, Fei W, Zhao Y, Wang F, Ye Y, Wang F. Combat against gynecological cancers with blood vessels as entry point: Anti-angiogenic drugs, clinical trials and pre-clinical nano-delivery platforms. *Int J Nanomedicine*. 2023;18:3035–3046. doi:10.2147/IJN.S411761.
 52. Baar J, Storkus WJ, Finke J, Butterfield L, Lazarus H, Reese J, Downes K, Budd T, Brufsky A, Fu P. Pilot trial of a type I - polarized autologous dendritic cell vaccine incorporating tumor blood vessel antigen-derived peptides in patients with metastatic breast cancer. *J Immunother Cancer*. 2015;33(S1):P3. doi:10.1186/2051-1426-3-S1-P3.
 53. Stapor PC, Sweat RS, Dashti DC, Betancourt AM, Murfee WL. Pericyte dynamics during angiogenesis: new insights from new identities. *J Vasc Res*. 2014;51(3):163–174. doi:10.1159/000362276.
 54. Meng MB, Zaorsky NG, Deng L, Wang H-H, Chao J, Zhao L-J, Yuan Z-Y, Ping W. Pericytes: a double-edged sword in cancer therapy. *Future Oncol*. 2015;11(1):169–179. doi:10.2217/fon.14.123.
 55. Firat H, Garcia-Pons F, Tourdot S, Pascolo S, Scardino A, Garcia Z, Michel M-L, Jack RW, Jung G, Kosmatopoulos K, et al. H-2 class I knockout, HLA-A2.1-transgenic mice: a versatile animal model for preclinical evaluation of antitumor immunotherapeutic strategies. *Eur J Immunol*. 1999;29(10):3112–3121. doi:10.1002/(SICI)1521-4141(199910)29:10<3112::AID-IMMU3112>3.0.CO;2-Q.
 56. Street MD, Doan T, Herd KA, Tindle RW. Limitations of HLA-transgenic mice in presentation of HLA-restricted cytotoxic T-cell epitopes from endogenously processed human papillomavirus type 16 E7 protein. *Immunology*. 2002;106(4):526–536. doi:10.1046/j.1365-2567.2002.01442.x.
 57. Angelakopoulos H, Loock K, Sisul DM, Jensen ER, Miller JF, Hohmann EL. Safety and shedding of an attenuated strain of *Listeria monocytogenes* with a deletion of actA/plcB in adult volunteers: a dose escalation study of oral inoculation. *Infect Immun*. 2002;70(7):3592–3601. doi:10.1128/IAI.70.7.3592-3601.2002.
 58. Maciag PC, Radulovic S, Rothman J. The first clinical use of a live-attenuated *Listeria monocytogenes* vaccine: a phase I safety study of Lm-LLO-E7 in patients with advanced carcinoma of the cervix. *Vaccine*. 2009;27(30):3975–3983. doi:10.1016/j.vaccine.2009.04.041.
 59. Tsujikawa T, Crocenzi T, Durham JN, Sugar EA, Wu AA, Onners B, Nauroth JM, Anders RA, Fertig EJ, Laheru DA, et al. Evaluation of cyclophosphamide/GVAX pancreas followed by *Listeria-mesothelin* (CRS-207) with or without nivolumab in patients with pancreatic cancer. *Clin Cancer Res*. 2020;26(14):3578–3588. doi:10.1158/1078-0432.CCR-19-3978.
 60. Mason NJ, Gnanandarajah JS, Engiles JB, Gray F, Laughlin D, Gaurnier-Hausser A, Wallecha A, Huebner M, Paterson Y. Immunotherapy with a HER2-targeting *Listeria* induces HER2-specific immunity and demonstrates potential therapeutic effects in a phase I trial in canine osteosarcoma. *Clin Cancer Res*. 2016;22(17):4380–4390. doi:10.1158/1078-0432.CCR-16-0088.
 61. Wallecha A, Malinina I, Molli P. *Listeria monocytogenes* (Lm)-LLO immunotherapies reduce the immunosuppressive activity of myeloid-derived suppressor cells and regulatory T cells in the tumor microenvironment. *J Immunother Cancer*. 2013;1(S1):468–476. doi:10.1186/2051-1426-1-S1-O18.